Electrically Driven Microengineered Bio-inspired Soft Robots

DOI: 10.1002/ ((please add manuscript number))

Electrically Driven Microengineered Bio-inspired Soft Robots

By *Su Ryon Shin[†]*, Bianca Migliori[†], Beatrice Miccoli, Yi-Chen Li, Pooria Mostafalu, Jungmok Seo, Serena Mandla, Alessandro Enrico, Silvia Antonia, Ram Sabarish, Ting Zheng, Pirrami Lorenzo, Yu Shrike Zhang, Kai-tak Wan, Demarchi Danilo, Mehmet R. Dokmeci, Ali Khademhosseini**

Dr. S.R. Shin, Dr. B. Migliori, B. Miccoli, Dr. Y.-C. Li, Dr. P. Mostafalu, Dr. J. Seo, S. Mandla, A. Enrico, S. Antona, R. Sabaish, T. Zheng, Dr. Y. S. Zhang. Dr. M.R. Dokmeci, Prof. A. Khademhosseini.
Biomaterials Innovation Research Center, Division of Engineering in Medicine, Brigham and Women's Hospital, Harvard Medical School, Boston, MA 02139, USA.
Harvard-MIT Division of Health Sciences and Technology, Massachusetts Institute of Technology, Cambridge, MA 02139, USA.
E-mail: SSHIN4@partners.org (S. R. Shin), alik@bwh.harvard.edu (A. Khademhosseini)

Dr. B. Migliori
Department of Neuroscience, Karolinska Institutet, 17177 Stockholm, Sweden.

Dr. B. Miccoli, P. Lorenzo and Prof. D. Danilo
Department of Electronics and Telecommunications, Politecnico di Torino, Torino, 10129, Italy.

P. Lorenzo
Department of Electrical Engineering, Institute for Printing, University of Applied Sciences and Arts Western Switzerland, Fribourg, 1705, Switzerland.

Dr. K.-t. Wan
Department of Mechanical and Industrial Engineering, Northeastern University, Boston, Massachusetts 02115, USA.

Prof. A. Khademhosseini.
Department of Physics, King Abdulaziz University, Jeddah 21569, Saudi Arabia.
Department of Maxillofacial Biomedical Engineering and Institute of Oral Biology, School of Dentistry, Kyung Hee University, Seoul, 130-701, Republic of Korea.

[†] S.R. Shin and B. Migliori contributed equally to this work.
[*] S.R. Shin and A. Khademhosseini contributed equally as corresponding authors.

Keywords: Hydrogels, Flexible microelectrode, Cardiac tissue engineering, Bio-inspired, Bio-actuator.

Abstract

Engineering bio-inspired living systems with the capacity to actuate in a biological environment is of interest for various biomedical applications, such as building biorobotics and implantable biosensors. Here, we report the development of a bio-inspired soft robotics system, with integrated self-actuating cardiac muscles on a hierarchically structured scaffold with flexible gold (Au) microelectrodes. Inspired by the unique and natural movement of living organism, we designed and fabricated a batoid ray-shaped scaffold, which was composed of two distinguished micro-patterned hydrogel layers. The first layer was a polyethylene glycol (PEG) hydrogel pattern, which stabilized the structure of the scaffold, followed by a layer of gelatin methacryloyl (GelMA) loaded with carbon nanotubes (CNT), which served as a cell culture substrate to improve maturation of cardiomyocytes. In addition, flexible Au microelectrode was embedded into the biomimetic scaffold for its excellent mechanical integrity and electrical conductivity. After culturing cardiomyocytes on the biomimetic scaffold, the resulting bio-inspired soft robot showed excellent myofiber organization and a unique self-actuating movement, which was directly related to the direction of the contractile force of the muscle tissue. The Au microelectrode allowed local electrical stimulation and control of the beating behavior of the bio-inspired soft robot.

1. Introduction

Engineered living-synthetic systems with the capacity to dynamically deform their shape and sense biological environments are of interest for various biomedical applications, such as building biorobotics, biosensors, and artificial muscles.[1, 2] In particular, to build these systems, a biological component is integrated on an artificial platform, regulated by dynamic control devices at the interface. The biological component provides functional capabilities, while the artificial system is used to ensure mechanical stability of the scaffold. Furthermore, the artificial system improves the functionality of the biological component, while ensuring

good biocompatibility.[3, 4-7, 8] In addition, the integration of dynamic control devices into biorobots will allow for stimulation of the biological component with specific activation patterns to improve their efficiency during long-term operation. Among various biological components, the advantages related to the use of living muscle have inspired the development of biomimetic constructs, including muscular thin film-based bio-hybrid actuators,[5] cantilevers,[6] walking "biological bimorph" bio-bots,[7] and self-propelled swimming robots.[8] Despite the significant advancements in this field, many limitations still remain, such as creating life-like movements, on-board control systems, robust actuation, and low power consumption of the biorobots.

To overcome these limitations, living muscle actuator technologies have taken notes from biomimetic concepts to develop bio-inspired robots. These biorobots are able to better mimic, and even overcome the performance of living organisms in some cases, thus opening new horizons in bio-robotic research. Moreover, natural mechanisms are generally sustainable, high performing, and energy-saving, which are important factors that should be addressed to tackle the issues within the current technology.[9] Specially, Parker et al., have developed multiple bio-inspired robots, such as the jellyfish-inspired robot[10] and the soft-robotic ray[2] using cardiomyocytes and elastomeric materials like polydimethylsiloxane (PDMS). However, micro-patterned PDMS has a high substrate rigidity, which has been known to affect the contractile function of cardiac tissue/cells, although, these few bio-inspired robots have successfully mimicked the movement of living organisms [11].

To achieve advanced soft biomimetic artificial systems, hydrogels from various components of the mammalian extracellular matrix (ECM) are more suitable material sources as they can allow for deformation, locomotion, and control of living muscle actuators to a greater degree of freedom. Furthermore, understanding and exploiting higher-dimensional micro-muscle assemblies is a key engineering and scientific challenge with immense potential. Structural and functional changes result when cardiac cell networks are cultured using a three-dimensional (3D) hydrogel scaffold topography. These changes include enhanced actin

cytoskeleton organization, higher nuclear eccentricity alterations to gene expression, protein localization, cell signaling, and intracellular calcium dynamics. These topology-induced changes are expected to enhance the orientation and beating functionality of cells. To induce elongation and orientation of the cardiac cells on the patterned surfaces, photolithography approaches combined with ECM-based biomaterials can be used to create the biomimetic micro-patterned surface in a convenient, rapid, accurate, repeatability, and inexpensive manner.[12] Furthermore, the incorporation of a controlling system, such as flexible electronic component, can provide users with precise control over their direction and behavior.[5, 13]

In this paper, we created a bio-inspired soft robot, modeled after a batoid ray. Batoid rays are cartilaginous fishes with dorsoventrally flattened bodies and extended pectoral fins. They can be easily mimicked by simplifying its structure and movements among various living organisms in ocean. Recently, Parker et al. developed a phototactic, guided soft-robotic ray using optogenetic control of the cardiomyocytes that replicates the overall fish morphology, and focused on mimicking a swimming behavior with undulatory locomotion.[2] However, various batoid rays exhibit different swimming styles that largely depend on their skeletal architecture (e.g., cartilage joint patterns), along with their aligned muscle tissues on their pectoral fins.[14] Consequently, here we are interested in mimicking the alignment of skeletal and musculature architectures of the batoid ray, which can modulate the movement of the robot. The cartilage structure and arrangement are key criteria to be considered in the design of an effective bio-inspired soft robot as it will have a strong influence on the kinematic motion of the robot.

Therefore, to mimic the features of a batoid ray, an engineered scaffold was designed by drawing inspiration from the biomechanical model of batoid rays with double muscle-like patterned layers composed of polyethylene glycol (PEG) and carbon nanotubes (CNTs)-gelatin methacryloyl (GelMA) hydrogels. In our previous work, we reported a GelMA hydrogel scaffold with homogeneously incorporated CNTs, which was shown to improve tissue organization, and cell-to-cell electrical coupling.[4] Cardiomyocytes cultured on the

CNT-GelMA hydrogels were found to spontaneously beat earlier than cells cultured on pristine GelMA, and maintained a stronger beating activity.[15, 16] Therefore, the CNT-GelMA micro-patterned hydrogel layer acts as a substrate for cell culture to induce maturation of the cardiac muscle cells. In addition, the encapsulation of nanomaterials, such as CNTs into the hydrogel, was demonstrated to be a suitable method to obtain the desired mechanical properties required to efficiently promote the integration of gold (Au) microelectrodes.[17, 18] Challenges arise when developing a soft-robotics system, as electrical components are typically brittle and fragile, whereas bio-inspired robots have a high elasticity and low elastic modulus. Therefore, the flexible Au microelectrode was designed to deform in line with the bio-inspired soft robot without cracking or disrupting the polymeric layers to successfully achieve the local electrical stimulation. The resulting muscle-like bio-inspired soft robot showed excellent mechanical integrity with the inserted micro-patterned Au electrode. Consequently, we successfully fabricated a bio-inspired soft robot with muscle-like patterns, and controllable motion under an electrical field produced by integrated flexible microelectrodes.

2. Results and Discussion

Design of bio-inspired soft robot

We designed and fabricated a bio-inspired soft robot, which combined the mechanical and biological properties of the batoid ray (**Figure 1**). The bio-inspired soft robot was composed of four layers: aligned muscle tissue, micro-patterned CNT-GelMA hydrogel, a flexible Au microelectrode, and a micro-patterned PEG hydrogel layer. The first layer, which aimed to mimic the structure and function of the cartilage joint patterns (blue dot in **Figure 1a**) of the skeletal architecture in a batoid ray, was composed of a PEG micro-patterned hydrogel (**Figure 1b**). In this case, the non-degradable, non-toxic, mechanically robust PEG hydrogel increased the stability of the structure, while the micro-pattern on the hydrogel allowed for easy deformation of the construct under cell contraction and relaxation when compared with a

thin PEG hydrogel film.[19] Furthermore, the PEG hydrogel acted as a supporting substrate to successfully integrate the Au microelectrode, allowing it to be easily transferred to the PEG hydrogel layer without ancillary sacrificial layers, which was developed in our previous study.[20, 21] For the second layer, a network of flexible Au microelectrodes was integrated into the scaffold to stimulate the robot with precise control and efficient electrical signal propagation along the robot. The nanometer-scale thin electrode was designed with a sinusoidal pattern, which helped to dissipate the physical stress of the metal electrode during muscle actuation when embedded in the scaffold.[22] The third layer was designed to mimic the directional muscle alignment against the cartilage joint patterns of the batoid ray. A CNT-GelMA micro-patterned hydrogel, which acts a biocompatible environment suitable for cardiomyocyte culture and alignment, was generated with a perpendicular pattern orientation to the PEG hydrogel pattern (**Figure S1**). Finally, the forth layer consisted of neonatal rat cardiomyocytes seeded on top of the CNT-GelMA hydrogel-patterned layer to obtain a batoid ray-shaped bio-inspired soft robot. After the maturation of the cardiomyocytes, the CNT-GelMA hydrogel pattern ensured contractions in the direction of cell alignment, while the PEG hydrogel pattern released membrane tension following contraction, thus allowing the scaffold to return to its original shape (**Figure 1c and d**). The detailed fabrication process of the bio-inspired soft robot with the incorporated flexible Au microelectrode is presented and schematically illustrated in the Supporting Information, **Figure S1.**

The spacing of the pattern is an important factor affecting cell alignment and cell-cell interactions between the hydrogel patterned lines, as reported in a previous study.[23] Three different pattern distances were test for both the PEG (200 μm, 300 μm, and 500 μm) and the CNT-GelMA (50 μm, 75 μm and 150 μm) hydrogels. To optimize these parameters, we fabricated a two-layer micro-pattern structure, 50 μm in width, where the CNT-GelMA hydrogel layer resided on top of the PEG hydrogel layer. The resultant scaffold is shown in **Figure 2a and b**, where the uniformly patterned perpendicular PEG and CNT-GelMA hydrogels can be clearly identified. The specific concentrations of GelMA (5 wt%) and CNT

(1 mg/ml) were selected to improve the maturation of the cardiac muscle tissue and cell-cell electrical coupling based on our previously published reports.[15, 21] As shown in the scanning electron microscopy (SEM) image (**Figure 2c**), the CNT-GelMA patterned hydrogel layer showed both fibrous networks, which could be attributed to the cross-linking of the GelMA-coated CNTs *via* the acrylic groups, and porosity distribution on its surface. This network structure is similar to the physical characteristic of collagen fibers in the native ECM.[15] The fibrous network promoted cell retention, maturation, attachment, and myotube striation (**Figure 2d**).[15] After cardiomyocyte seeding, strong interconnected networks with partial alignment in the direction of the hydrogel pattern were observed from the F-actin expression in the conditions with a denser CNT-GelMA hydrogel pattern (50 and 75 μm). On the contrary, clear and precise cell alignment on the CNT-GelMA hydrogel pattern was noticed on scaffolds with 150-μm spacing (**Figure 2e**). Despite the inferior cell alignment, the spontaneous beating had a higher frequency and was more constant on the 75-μm spacing (frequency: 0.88 ± 0.07 Hz) than on the 50-μm spacing (frequency: 0.53 ± 0.24 Hz) and the 150-μm spacing (frequency: 0.24 ± 0.07 Hz) (**Figure 2f and g**). This could be related to the higher number of cell-cell interactions, which led to the higher beating synchronization and frequency.[24] The reported results are in agreement with our previous study, in which the beating behavior was highly correlated to the cellular connections and interaction.[15]. After identifying the 75-μm spacing as the optimal CNT-GelMA hydrogel pattern to induce strong beating behavior (**Video 1**), the cytotoxicity of the scaffold was further assessed, showing an increase in cell viability over a period of 7 days (**Figure 2h)**. These results confirmed that the CNT-GelMA patterned hydrogels are not cytotoxic to the cardiac cells and are capable of inducing proliferation of cardiac fibroblasts.

To increase the stability of the structure and to allow the soft robot to properly recover to its original shape after cardiomyocyte contraction, the concentration of the PEG hydrogel was optimized to 20 wt%. This choice represents a tradeoff between high-weight percent PEG

hydrogels (>30 wt%), which were too stiff to allow for scaffold contraction upon cell contraction, and low-weight percent PEG hydrogels (<10 wt%), which were unable to counteract the contractile cell traction forces that originate from actin polymerization and actomyosin interactions.[25] Therefore, it can provide robust mechanical properties to increase the stability of the soft robot construct, while the micro-pattern of the PEG hydrogel allows for easy deformation of the construct under cell contraction and relaxation when compared to a thin PEG hydrogel film. Furthermore, the geometry of the supporting PEG hydrogel pattern dramatically affects the function of the bio-inspired soft robot in terms of both directional beating and overall structure folding. To prevent an irreversible complete rolling of the soft robot during the beating dynamics of the cardiomyocytes, the pattern spacing of the PEG hydrogel support layer was varied between 200, 300 and 500 μm (**Figure 2h**). As expected, the pattern density of the PEG hydrogel strongly influenced the bio-inspired actuator kinematics. The bio-inspired actuator without PEG hydrogel pattern was spontaneously rolled up and showed strong beating behavior (**Video 2**). In the case of the 200-μm spacing, no folding of the overall structure was observed, due to the high density of the PEG hydrogel pattern; however, it was too stiff to allow for the bending of the soft robot upon cardiomyocyte contraction (**Video 3**). On the contrary, a strong and irreversible rolling of the bio-inspired actuator was observed and showed weak beating behavior when the PEG hydrogel pattern was spaced by 500 μm, thus compromising the actuation dynamics of the soft robot (**Video 5**). A middle ground for the PEG hydrogel pattern density was found to be at 300 μm. In this condition, the supporting PEG hydrogel layer was soft enough to follow the cardiomyocyte-induced bending of the soft robot, while remaining sufficiently stable to prevent an irreversible folding of the scaffold. Therefore, we introduced a specific score index to evaluate the optimal spacing of both the CNT-GelMA and PEG hydrogel layers to simultaneously obtain a strong synchronized beating behavior and prevent the irreversible rolling of the bio-inspired actuator (**Figure 2i**). The index consisted of the sum of a “rolling score” (0 in the case of no rolling, -1 in the case of rolling) and a “beating level” varying from

0, in the case of no beating, to 3, in the case of very strong beating. The highest score index was obtained for a PEG and CNT-GelMA hydrogel pattern with a spacing of 300 μm and 75 μm, respectively, which led to the optimal beating and actuation dynamics of the soft robot (**Video 4**).

2.2 Cell beating behavior on the scaffold

After seeding neonatal rat cardiomyocytes on the optimized soft robot with CNT-GelMA and PEG hydrogels pattern distance of 75 μm and 300 μm, respectively, the cells were stained for specific cardiac biomarkers, including sarcomeric α-actinin, and connexin-43 (Cx-43)[26] to observe the tissue morphology and phenotype. Notably, in the case of the 75-μm CNT-GelMA hydrogel spacing, cardiomyocytes on the top layer were observed to show alignment along the CNT-GelMA hydrogel pattern, and were interconnected between the patterned lines (**Figure 3a and b**), leading to the formation of a pseudo-3D cardiac tissue construct. More specifically, as shown in the schematic in **Figure 3a**, and confirmed by confocal fluorescent microscopy, a homogeneous distribution of Cx-43, and well-organized sarcomeric α-actinin structures were observed on the topmost tissue (**Figure 3b (i)-(ii)**). This tissue is primarily responsible for the synchronous beating of the whole construct. Alternatively, in the intermediate and bottom layers (**Figure 3b (iii)-(iv)**) sarcomeric α-actinin expression resulted in partially aligned and organized tissue along the muscle-like hydrogel structure, which was found to not only enhance the synchronous contractile properties of the structure but also to guide the actuation dynamics parallel to the direction of the CNT-GelMA hydrogel pattern (**Figure 3a**) i.e., inducing the swimming-like movement of the bio-inspired soft robot.

The soft robot showed spontaneous and synchronous beating when neonatal rat cardiomyocytes were cultured on the biomimetic scaffold starting at day 3 (beating frequency 0.99 ± 0.08 Hz), until day 9 (beating frequency 0.82 ± 0.11 Hz), with no significant frequency reduction (**Figure 3c**). Interestingly, because of the patterned design of the PEG hydrogel

substrate, the cultured cardiomyocytes on the biomimetic multilayer scaffold showed a similar beating rate compared to those on pristine CNT-GelMA hydrogels as shown in our previous work.[15] Consequently, the optimized micro-patterned PEG hydrogel did not inhibit the cardiac muscle actuation on the scaffold. Moreover, the strong spontaneous beating behavior of the cardiomyocytes naturally induced the detachment of the scaffold from the supporting glass 4 or 5 days into the culture period, as shown in **Figure 3d and Video 4**. The rolling behavior of the edges on the lateral patterned fins was due to the cellular traction force along the CNT-GelMA hydrogel pattern, i.e., in the transverse direction.

Finally, the obtained bio-inspired soft robot showed a unique self-actuating movement. In **Figure 3d and e**, a longitudinal (blue line, stretching) and transverse (green line, contracting) axes on the soft robot showed an opposite direction of actuation at the same time. A much higher contraction of the laterally patterned fins was observed in the transverse axes of the soft robot due to the strong muscle contraction of the aligned cardiac tissue along the CNT-GelMA hydrogel pattern (**Figure 3b (iii) and (iv)**). In addition, the micro-pattern of the stiff PEG hydrogel with a spacing of 300 μm may help to induce the easy deformation of the micro-patterned soft CNT-GelMA hydrogel under cell contraction. To confirm the mechanical properties of two micro-patterned hydrogels, we performed a nano-indentation test.[27] The Young's modulus, derived from the force indentation data using a Hertzain model, of the micro-patterned PEG hydrogel was 651.0 ± 326.0 kPa which was 30 times higher than that of the CNT-GelMA hydrogel (37.1 ± 16.5 kPa) as shown in **Figure 3f**. On the contrary, the soft robot showed less deformation in the longitudinal axes (blue dot line), i.e., in the direction of the PEG hydrogel pattern. The longitudinal displacement can be mainly attributed to the 60° angle of the CNT-GelMA pattern with respect to the main axes of the soft robot that induce a force component in the vertical direction (**Figure 3g**). Furthermore, the contraction of the topmost of the cardiac tissue (**Figure 3b (i) and (ii)**) produced a stress on the underlying PEG hydrogel layer, which relaxed by elongating in the opposite direction.

This movement is more evident in the tail section due to the absence of the central body, which dampens the displacement due to higher stiffness of the PEG hydrogel. After one full contraction, the bio-inspired actuator returns to the original rest position because of the elastic response provided by the PEG hydrogel pattern. These assumptions are confirmed by the results of the actuation dynamics and the particle velocimetry analysis of the soft robot from 0 to 0.3 sec as shown in **Figure 3d (ii)**. To assess the ability to control the soft robot by electrical stimulation, a specific square wave electrical signal was applied to the soft robot to tune and artificially control the beating behavior through commercially available carbon rod electrodes as commonly reported in literature.[28] As outlined in **Figure 3h**, the overall beating frequency of the soft-robot was precisely controlled at different frequencies (0.5, 1 and 2 Hz), by stimulation through a square wave signal with a frequency equal to the target beating frequency, AC peak voltage between 0.5 V and 6 V, 0V DC, a fixed pulse width of 50 ms and Duty Cycle of 2.5%, 5% and 10% in case of 0.5, 1 and 2 Hz, respectively .

2.3 Incorporation of the Au microelectrode in the scaffold

The local control of the electrical stimulation of the soft robot was achieved through the encapsulation of a network of 200-nm-thick Au microelectrodes in the structure. The Au microelectrodes (**Figure 4a**) were deposited on a glass substrate by e-beam evaporation (see the Experimental Section for further details). Atomic force microscopy (AFM) characterization (**Figure 4b**) revealed a root mean square (RMS) roughness of 2.00 ± 0.44 nm, therefore providing compelling evidence of the high quality of the deposited electrode. The shape of the embedded Au microelectrodes was designed to allow the structure to maintain a high degree of flexibility necessary for the microelectrodes to not impede the beating cardiomyocytes, and to favor an optimal electric field distribution across the scaffold, such that a wave-like displacement (arc segment angles: 120°), originating from the central region of the structure can be achieved.

Direct UV crosslinking of the PEG and CNT-GelMA hydrogels on the surface of the microelectrodes not only prevented electrode delamination, but also allowed the microelectrodes to be directly incorporated between the two hydrogels. Successful transfer and encapsulation of the microelectrodes in the PEG hydrogels, was assessed using SEM (**Figure 4c and 4d**) to ensure that there were no cracks at the interface between the microelectrodes and the hydrogel or surface damage of the microelectrodes. The Au electrode was then completely enclosed in the micro-patterned CNT-GelMA hydrogel, which was assessed using optical imaging, as shown in **Figure 4e**. It was confirmed experimentally that the Young's modulus of the micro-patterned CNT-GelMA hydrogel on the Au electrode was similar to that of the micro-patterned CNT-GelMA hydrogel only. Therefore, the CNT-GelMA hydrogel was successfully deposited on top of the Au microelectrodes; however, the Au electrode may have partially inhibited the crosslinking of the CNT-GelMA prepolymer under the microelectrodes as the UV light could not penetrate the Au electrode. Finally, we obtained the bio-inspired soft robot with an embedded Au microelectrodes between the hydrogel layers as shown in **Figure 4f**. To further assess the stability of the electrodes in cell culture condition, its resistance was monitored for 5 days of incubation in cell culture media at 37 °C, (**Figure 4g**). Only a slight relative variation of resistance (between a minimum value of 0.009 ± 0.018 a.u. and a maximum value of 0.023 ± 0.004 a.u.) was observed during the 5 days of culture, thus confirming the stability and cohesion of the electrode in the biological environment.

In addition, the modulus of the electrical impedance was measured for the transferred microelectrodes on the PEG hydrogel layer, the encapsulated microelectrode within two hydrogel layers, and the entire soft robot with cultured cardiomyocytes (**Figure 4h**). As expected, at frequencies higher than 0.1 kHz, the presence of the capacitive current strongly decreases the modulus of the impedance on the PEG/microelectrodes (from 630.00 Ω to 251.00 Ω between 0.12 and 82.52 kHz), PEG/microelectrodes/CNT-GelMA (from 280.00 Ω

to 61.00 Ω between 0.12 and 82.52 kHz) and PEG/microelectrodes/CNT-GelMA/cardiomyocytes (from 317.50 Ω to 88.59 Ω between 0.12 and 82.52 kHz) samples. Alternatively, at lower frequencies that are more representative of physiological conditions, an impedance modulus reduction could be observed when the CNT-GelMA hydrogel layer was added on the PEG/microelectrodes structure (from 2.3 to 1.6 kΩ at 0.1 Hz). This can be attributed to the presence of additional current paths through the CNTs incorporated in the GelMA hydrogel, and will therefore contribute to an efficient electrical signal propagation through the cardiomyocytes. When cardiomyocytes were seeded on the soft robot with the embedded Au microelectrodes, a moderate impedance modulus increase was noticed, likely due to the intrinsic resistivity of the cells. Moreover, to confirm the organization of cardiac tissue on the microelectrodes-incorporated soft robot, immunostaining of sarcomeric α-actinin and F-actin was investigated. As shown in **Figure 4i and 4j**, we observed the random network formation of cardiac tissue with well-interconnected sarcomeric structures on the central body due to the absence of a pattern on the CNT-GelMA hydrogel (**Figure 4i and 4j**). In addition, well-interconnected sarcomeric structures of cardiac tissues located directly above the microelectrodes (**Figure S2a**) were observed. On the contrary, the cardiomyocytes were only partially aligned with the micro-patterned CNT-GelMA hydrogel on the lateral patterned fins, as evident from **Figures 4k and 4l** (confocal microscope characterization using sarcomeric α-actinin and connexin-43 was also performed and it can be observed in **Figure S3**).

2.4 Electrophysiological analysis of the bio-hybrid actuator

After cardiomyocytes seeding, the bio-hybrid construct with the embedded Au microelectrodes could efficiently maintain its original shape and integrity during the culture period (**Figure 5a**). Moreover, to make use of the embedded microelectrodes, two copper wires were joined to the outermost end of the electrode to electrically stimulate the bio-inspired actuator. The joint was insulated from the culture media by a thin layer of PDMS

(**Figure 5a**). To investigate how an external voltage signal propagates and distributes along the construct, finite element model simulations were performed using commercially available software, both in the case of the embedded microelectrodes or an external carbon rod electrode. When a square wave signal (AC peak amplitude 1V, 0V DC, frequency 2 Hz, period 50 ms, Duty Cycle 10%) was simulated in the case of the microelectrode, the maximum voltage intensity was 1 V in the central area of the structure (**Figure 5b**). The observed non-uniform electric potential distribution suggested a non-simultaneous electrical excitation of the cardiomyocytes. This can result in a wave-like displacement of the whole structure, in which the movement originates from the central body, and propagates towards the outer fin regions. On the contrary, the external carbon rod electrode simulation results revealed an almost uniform voltage distribution along the entire structure (**Figure S4b**). This implies that the different areas of the scaffold will contract at the same time producing a defined on/off displacement, which is not similar to the movement of a batoid ray. Moreover, during the simulation with the external carbon electrodes, the stimulation voltage peak was increased from 1 V to 4 V to take into account the signal dispersion in the cell culture media. As a result, the actual signal reaching the scaffold had peak amplitude of only 2 V, while, in the case of the microelectrode stimulation, the entire applied signal propagated through the core of the structure. This underlines how the local microelectrodes could offer improved stimulation efficiency.

To control the beating frequency of the soft robot at a specific target frequency (0.5, 1 and 2 Hz), a square waveform at various frequencies (pulse width: 50 ms, Duty Cycle: from 2.5% to 10%, peak voltage amplitude: from 0.5 to 6 V, DC value: 0V, Frequency: 0.5, 1 and 2 Hz) was applied to both microelectrodes. In the case of the external carbon rod electrodes, full synchronization was obtained with relatively low excitation peak voltages, ranging from 0.8 ± 0.22 to 1.5 ± 0.02 V (**Figure 5c and S5a**). When the excitation frequency was increased from 0.5 to 2 Hz, the excitation threshold voltage also increased. This trend may be attributed to the

slower actuation dynamics at the cellular level, which is limited by the repolarization and diffusion of nutrients from the ionic pumps. The same measurements were repeated in the case of local stimulation. The obtained excitation threshold voltage was slightly higher than the one obtained in the case of the external carbon rod electrode stimulation. Nevertheless, we successfully tuned the beating behavior of the cardiomyocytes at 0.5 and 1 Hz, as shown in **Figure 5c**. However, we were unable to achieve a stimulation frequency of 2 Hz, as the artificial tuning of the beating behavior could not be achieved for peak amplitudes smaller than 3 V, which was the maximum waveform amplitude we could apply. This indicates that much higher waveform amplitudes should be applied to the system (**Figure S5b**).

The increase of excitation threshold required for the embedded Au microelectrodes may be attributed to the simultaneous action of two antagonist electrical phenomena. The first is that we expect the overall system resistance to increase with the embedded microelectrodes as a result of its smaller dimensions in comparison to the carbon electrodes. Second, during the local stimulation, the electrical signal was spatially closer, and almost coincident, with the cells rather than at a centimeter-scale distance away from the external electrodes. A smaller dielectric layer could thus be hypothesized in the case of embedded microelectrodes, i.e., a lower voltage drop between the electrode surface and the cells in favor of the effective potential present at the junction. Although the first effect should be predominant, the second could strongly contribute to mitigate it, maintaining the excitation threshold to relatively small values, of below 3 V, as experimentally observed. The tradeoff between these two phenomena allowed the embedded microelectrodes to efficiently and locally stimulate the bio-inspired soft robot. Finally, to evaluate the viability of cardiac tissues after local electrical stimulation, the spontaneous beating frequency was recorded (**Video 6**). As shown in **Figure 5d**, the spontaneous beating was almost unaffected, regardless of the multiple electrical stimulations with different modulations, performed for 4-5 h. These results revealed that the microelectrode incorporation and the electrical tests produced only a negligible wear on the cell integrity, i.e., the beating behavior was still similar, and of the same order of magnitude to

that observed when no electrode was present (**Figure 3c**). The obtained results strongly supported the concept that a bioinspired soft-robot could successfully control the beating frequency using embedded Au microelectrodes without damaging the cardiac tissues.

Recently, Parker *et al.* published a pioneer work on a PDMS-based soft-robotic phototactic ray guided with optogentics[2], in which they focused on the motion dynamics as opposed to mimicking the fish cartilage-muscle structure, which is the main thrust of our work. In addition, our study has focused on developing an electrical stimulation system, instead of using genetically engineered optogenetic method. Therefore, our method is potentially simpler and more versatile, and may eventually lead to a wireless electrical stimulation system for production of bio-inspired soft robotics in the future. Moreover, instead of PDMS, we selected a nanomaterial-incorporated hybrid hydrogels with the ability to simultaneously mimicking the ECM components, while still showing excellent electromechanical properties. The CNT-GelMA hydrogel is more favorable for cell proliferation and maturation, and allows for a more emphasized life-like actuation dynamics as a result of its softer properties. Consequently, both methods present their own advantages and disadvantages, but the system we established with an embedded flexible microelectrode in the biomimetic hydrogel will offer a reliable alternative strategy building the development of a bioinspired soft-robot.

3. Conclusions

In summary, we have developed a bio-inspired soft robotics system, with integrated self-actuating cardiac myofibers on a hierarchically structured scaffold with flexible Au microelectrodes. The bio-inspired scaffold was sucessfully fabricated by mimicking of the biomechanical model of batoid rays, that is composed of two distinguished micro-patterned hydrogel layers with PEG and CNTs-GelMA hydrogels. The cells were seeded on a CNT-GelMA hydrogel pattern overlying a PEG patterned hydrogel, with a Au microelectrode incorporated between the two materials. The bio-inspired scaffold showed good mechanical

stability and ideal conditions for cell organization and maturation, as a result of the presence of ECM components in the CNT-GelMA hydrogel. High viability during cell seeding was followed by spontaneous beating along the CNT-GelMA hydrogel pattern until day 7 of culture. Staining on day 5 revealed partial uniaxial alignment of sarcomeric α-actinin in the cells along the CNT-GelMA hydrogel pattern. The electrical stimulation of the bio-inspired actuator was performed using both external carbon rod electrodes as well as local embedded micrometer-size Au electrodes. Although local stimulation featured higher excitation voltage thresholds with respect to external stimulation, in both cases it was possible to control the beating up to a frequency of 1 Hz, regardless of the natural beating frequency, by applying peak voltages smaller than 3 V. The valuable results obtained in the present work not only encourage further developments in the field of bio-inspired actuators but also serve as an initial platform for new, cutting-edge studies on local electrical stimulation of scaffolds with embedded microelectrodes for use as a wireless control system of the whole scaffold. Therefore, microfabricated cell-based hybrid actuators have the potential to greatly enhance the performance of biorobotics and potentially result in cheaper, faster, and easier-to-use analytical tools that are more portable and scalable for point-of-care sample analysis and real-time diagnosis.

4. Experimental section

Materials: The following reagents were purchased from Sigma-Aldrich (USA): Gelatin (Type A, 300 bloom from porcine skin), polyethylene glycol diacrylate (PEGDA) (M_W=1000), 3-(trimethoxysily) propyl methacrylate (TMSPMA), and methacrylic anhydride (MA). A carboxyl acid group functionalized multi-walled CNT (30 ± 15 nm in diameter and 5-20 μm length, 95%purity) was purchased from NanoLab Inc. The photo mask for the soft lithography and the shadow mask for the physical vapor deposition (PVD) process of the electrode patterning was purchased from CAD/Art Services, Inc. (USA) and from MINI MICRO STENCIL INC. (USA).

Preparation of the bio-inspired soft robot: The fabrication process is illustrated in Supporting **Figure S1**. First, the 200-nm-thick Au microelectrode with the desired wavy shape was fabricated on a glass substrate using the shadow mask by e-beam evaporation. Both the shadow mask for the Au microelectrode and the photomask used to fabricate the PEG and CNT-GelMA hydorgel patterns were designed using AutoCAD (Autodesk Inc., San Rafael, CA). The Au microelectrodes were then transferred onto the PEG hydrogel pattern by dispensing 10 μL of 20% PEG pre-polymer solution onto the Au microelectrode substrate, and TMSPMA coated glass was placed on top. The first photomask was interposed between the hydrogel and the UV light to produce the micro-pattern, and a spacer of 50 μm was placed between the electrode and the TMSPMA coated glass to produce a desired thickness of 50 μm for the PEG hydrogel layer. The pre-polymer solution was then cured by UV light (25.6 mW/cm^2) for 120 sec. By peeling the TMSPMA coated glass from the Au electrodes substrate, we successfully obtained the Au microelectrodes embedded in the micro-patterned PEG hydrogel. The Au microelectrodes embedded in the micro-patterned PEG hydrogel was then placed on top of 20 μL of CNT-GelMA pre-polymer solution (with a 100 μm spacer) and UV crosslinked (25.6 mW/cm^2) for 240 sec with the second photomask. CNT-GelMA (1.0 mg/ml CNT in 5% GelMA) and PEG hydrogels were prepared based on our previously published reports.[15, 29]

Characterization of the bio-inspired soft robot: A scanning electron microscope (SEM, Hitachi Model S4700, Japan) was used to assess the structure of the CNT-GelMA hydrogel. The samples were frozen in liquid nitrogen, then lyophilized, and finally coated with Pt/Pd using a sputter coater for SEM imaging. To measure the mechanical propertiesy of micro-patterned hydrogels, we performed AFM-assisted nano-indentation which was established in our published study.[30] The impedance modulus of the Au microelectrode at different

intermediate fabrication steps was measured using an electrochemical workstation CHI660E (CH instrument, Inc.). We used an Ag/AgCl electrode as a reference electrode and Pt sheet as counter electrode along with Au microelectrode as the working electrode. For the electrochemical impedance spectroscopy technique, the initial peak potential was set to 0.1 V and the range of frequencies were scanned from 0.1 Hz to 100 kHz at 5 mV of peak amplitude. All measurements were carried out in phosphate-buffered saline (PBS).

Cardiomyocytes isolation and culture: The cardiomyocytes were isolated from the heart ventricles of neonatal rats (2 days old Sprague-Dawley) following protocols approved by the Institute's Committee on Animal Care for isolation.[18] The cells were cultured in Dulbecco's modified eagle medium (DMEM, ThermoFisher, USA) with 10% fetal bovine serum (FBS, ThermoFisher, USA), 1% L-glutamine, and 100 units/mL penicillin-streptomycin (ThermoFisher, USA).

Cell characterization: To access the viability of cardiomyocytes on the scaffold, an Alamar Blue assay (ThermoFisher, USA) was performed using the manufacturer's suggested protocol. The samples were analyzed on day 1, 3, 5, and 7 after cell seeding and the considered wavelength of absorption was 570 nm. For immunostaining, samples were fixed in 4% paraformaldehyde for 20 minutes and washed with PBS at room temperature. The samples were then treated in 0.15% Triton X-100 in PBS for 10 minutes. The samples were incubated with a cardiac biomarker (sarcomeric α-actinin and connexin-43 (Abcam, USA)) in the presence of a blocking buffer for 45 minutes at room temperature following the manufacturer's suggested dilution. Then, the samples were counterstained with DAPI (Sigma, USA) at a dilution of 1:1000 in PBS for an additional 20 minutes. The sample were also treated with Alexa Fluor 488 phalloidin (1:40 dilution in PBS) and DAPI for 40 minutes at room temperature. An inverted fluorescence microscope (Nikon, Eclipse TE 2000U, Japan)

and an Inverted laser scanning confocal microscope (Leica SP5X MP, Germany) were used to obtain the cellular fluorescent images.

Actuation assessment of the bio-inspired soft robot: From day 1 to day 5, the bio-inspired actuators were incubated at 37 °C and imaged daily using an inverted optical microscope (Nikon, Eclipse TE 2000U, Japan). Once the cardiomyocytes began to show a beating activity (normally at day 3), the cell movements were recorded using video capture software at 20 frames per second (20 fps). By day 5, the bio-inspired actuator was detached from the TMSPMA coated glass. The sample was then placed in-between the two carbon rod electrodes spaced 3 cm apart in the culture media. The actuators were then stimulated by applying a square waveform with 50 ms pulses width, DC 0V and a peak amplitude between 0.5–6 V. The frequency was varied between 0.5, 1 and 2 Hz with a duty cycle between 2.5, 5 and 10%, respectively. The resulting beating activity was recorded using a commercially available camera. A custom developed MATLAB® code (MathWorks Inc., Natick, MA) was written to measure the bio-inspired actuator displacement along the selected directions. The local electrical stimulation *via* the Au microelectrode was carried out both for samples adhering to the glass substrate and for the detached samples. To deliver the electric signal directly on the internal Au electrode, two copper wires were attached to the Au electrode external square ports using silver paste. The silver paste was covered with a thin layer of PDMS pre-cured in the oven for 5 minutes. The PDMS was cured completely by placing the sample on a hotplate set at 45 °C for about 5 hours. The bio-inspired actuator was then electrically stimulated and tested by applying a square wave with an offset voltage, V_{OFF}, set to 1 V and the amplitude, V_{ON}, was varied between1.5 V and 5 V. For each of these conditions, stimulation frequencies of 0.5, 1 and 2 Hz were tested. The simulation of the propagation of the applied electrical signal through the structure with both the external and embedded Au microelectrodes was evaluated using COMSOL Multiphysics® electrostatic module (COMSOL Inc.), see Supporting Information for further details.

Statistical analysis: Statistical significance was performed by measuring one-way ANOVA tests (GraphPad Prism 5.02, GraphPad Software). To analyze and assess significant differences between selected treatments, Tukey's multiple comparison tests were utilized. Differences were characterized as significant for $p < 0.05$.

Acknowledgements

The authors declare no conflict of interests in this work. The authors gratefully acknowledge funding by the Defense Threat Reduction Agency (DTRA) under Space and Naval Warfare Systems Center Pacific (SSC PACIFIC) Contract No. N66001-13-C-2027. The authors also acknowledge funding from the Office of Naval Research Young National Investigator Award, the National Institutes of Health (EB012597, AR057837, DE021468, HL099073, R56AI105024), the Presidential Early Career Award for Scientists and Engineers (PECASE), and Air Force Office of Sponsored Research under award # FA9550-15-1-0273. This work was partially supported by a microgrant from Brigham Research Institute and Center for Faculty Development and Diversity's Office for Research Careers at Brigham and Women's Hospital. S.R.S. would like to recognize and thank Brigham and Women's Hospital President Betsy Nabel, MD, and the Reny family, for the Stepping Strong Innovator Award through their generous funding. Y.S.Z. acknowledges supports from the National Cancer Institute Pathway to Independence Award (K99CA201603).

Supporting Information

Supporting Information is available from the Wiley Online Library or from the author.

Received: ((will be filled in by the editorial staff))

Revised: ((will be filled in by the editorial staff))

Published online: ((will be filled in by the editorial staff))

References

[1] M. T. Holley, N. Nagarajan, C. Danielson, P. Zorlutuna, K. Park, Lab Chip 2016, 16, 3473.
[2] S. J. Park, M. Gazzola, K. S. Park, S. Park, V. Di Santo, E. L. Blevins, J. U. Lind, P. H. Campbell, S. Dauth, A. K. Capulli, F. S. Pasqualini, S. Ahn, A. Cho, H. Yuan, B. M. Maoz, R. Vijaykumar, J. W. Choi, K. Deisseroth, G. V. Lauder, L. Mahadevan, K. K. Parker, Science 2016, 353, 158.
[3] H. Herr, R. G. Dennis, Journal of NeuroEngineering and Rehabilitation 2004, 1; C. Cvetkovic, R. Raman, V. Chan, B. J. Williams, M. Tolish, P. Bajaj, M. S. Sakar, H. H. Asada, M. T. A. Saif, R. Bashir, Proceedings of the National Academy of Sciences of the United States of America 2014, 111, 10125; J. C. Nawroth, H. Lee, A. W. Feinberg, C. M. Ripplinger, M. L. McCain, A. Grosberg, J. O. Dabiri, K. K. Parker, Nature Biotechnology 2012, 30, 792; J. Kim, J. Park, S. Yang, J. Baek, B. Kim, S. H. Lee, E. S. Yoon, K. Chun, S. Park, Lab on a Chip - Miniaturisation for Chemistry and Biology 2007, 7, 1504.
[4] S. R. Shin, S. M. Jung, M. Zalabany, K. Kim, P. Zorlutuna, S. B. Kim, M. Nikkhah, M. Khabiry, M. Azize, J. Kong, K. T. Wan, T. Palacios, M. R. Dokmeci, H. Bae, X. Tang, A. Khademhosseini, ACS Nano 2013, 7, 2369.
[5] A. W. Feinberg, A. Feigel, S. S. Shevkoplyas, S. Sheehy, G. M. Whitesides, K. K. Parker, Science 2007, 317, 1366.
[6] J. Xi, J. J. Schmidt, C. D. Montemagno, Nat Mater 2005, 4, 180.
[7] V. Chan, K. Park, M. B. Collens, H. Kong, T. A. Saif, R. Bashir, Sci Rep 2012, 2, 857; V. Chan, J. H. Jeong, P. Bajaj, M. Collens, T. Saif, H. Kong, R. Bashir, Lab Chip 2012, 12, 88.
[8] B. J. Williams, S. V. Anand, J. Rajagopalan, M. T. Saif, Nat Commun 2014, 5, 3081.
[9] D. Rus, M. T. Tolley, Nature 2015, 521, 467.
[10] J. C. Nawroth, H. Lee, A. W. Feinberg, C. M. Ripplinger, M. L. McCain, A. Grosberg, J. O. Dabiri, K. K. Parker, Nat Biotechnol 2012, 30, 792.
[11] M. L. McCain, A. Agarwal, H. W. Nesmith, A. P. Nesmith, K. K. Parker, Biomaterials 2014, 35, 5462.
[12] R. S. Kane, S. Takayama, E. Ostuni, D. E. Ingber, G. M. Whitesides, Biomaterials 1999, 20, 2363; Y. N. Xia, G. M. Whitesides, Angewandte Chemie-International Edition 1998, 37, 551; A. Khademhosseini, S. Jon, K. Y. Suh, T. N. T. Tran, G. Eng, J. Yeh, J. Seong, R. Langer, Advanced Materials 2003, 15, 1995; K. Y. Suh, A. Khademhosseini, J. M. Yang, G. Eng, R. Langer, Advanced Materials 2004, 16, 584; G. M. Whitesides, E. Ostuni, S. Takayama, X. Y. Jiang, D. E. Ingber, Annual Review of Biomedical Engineering 2001, 3, 335.
[13] Z. Jia, V. Valiunas, Z. Lu, H. Bien, H. Liu, H. Z. Wang, B. Rosati, P. R. Brink, I. S. Cohen, E. Entcheva, Circ Arrhythm Electrophysiol 2011, 4, 753.
[14] R. S. Russo, S. S. Blemker, F. E. Fish, H. Bart-Smith, Bioinspiration & biomimetics 2015, 10, 046002.
[15] S. R. Shin, S. M. Jung, M. Zalabany, K. Kim, P. Zorlutuna, S. B. Kim, M. Nikkhah, M. Khabiry, M. Azize, J. Kong, K. T. Wan, T. Palacios, M. R. Dokmeci, H. Bae, X. S. Tang, A. Khademhosseini, ACS Nano 2013, 7, 2369.
[16] S. R. Shin, B. Aghaei-Ghareh-Bolagh, X. Gao, M. Nikkhah, S. M. Jung, A. Dolatshahi-Pirouz, S. B. Kim, S. M. Kim, M. R. Dokmeci, X. S. Tang, A. Khademhosseini, Adv Funct Mater 2014, 24, 6136.
[17] T. Dvir, B. P. Timko, M. D. Brigham, S. R. Naik, S. S. Karajanagi, O. Levy, H. Jin, K. K. Parker, R. Langer, D. S. Kohane, Nature Nanotechnology 2011, 6, 720; S. R. Shin, H. Bae, J. M. Cha, J. Y. Mun, Y. C. Chen, H. Tekin, H. Shin, S. Farshchi, M. R. Dokmeci, S. Tang, A. Khademhosseini, ACS Nano 2012, 6, 362; A. S. Blum, C. M. Soto, K. E. Sapsford, C. D. Wilson, M. H. Moore, B. R. Ratna, Biosensors and Bioelectronics 2011, 26, 2852; I. Rajzer, M. Rom, E. Menaszek, P. Pasierb, Materials Letters 2014, 138, 60; P. Baei, S. Jalili-

Firoozinezhad, S. Rajabi-Zeleti, M. Tafazzoli-Shadpour, H. Baharvand, N. Aghdami, Materials Science and Engineering C 2016, 63, 131.
[18] S. R. Shin, C. Shin, A. Memic, S. Shadmehr, M. Miscuglio, H. Y. Jung, S. M. Jung, H. Bae, A. Khademhosseini, X. Tang, M. R. Dokmeci, Advanced Functional Materials 2015, 25, 4486.
[19] Y. Wang, R. Yang, Z. Shi, L. Zhang, D. Shi, E. Wang, G. Zhang, ACS Nano 2011, 5, 3645; S. Sharifi, S. B. Blanquer, T. G. van Kooten, D. W. Grijpma, Acta Biomater 2012, 8, 4233.
[20] B. Tian, J. Liu, T. Dvir, L. Jin, J. H. Tsui, Q. Qing, Z. Suo, R. Langer, D. S. Kohane, C. M. Lieber, Nat Mater 2012, 11, 986.
[21] S. R. Shin, C. Shin, A. Memic, S. Shadmehr, M. Miscuglio, H. Y. Jung, S. M. Jung, H. Bae, A. Khademhosseini, X. S. Tang, M. R. Dokmeci, Advanced Functional Materials 2015, 25, 4486.
[22] P. Gutruf, S. Walia, M. N. Ali, S. Sriram, M. Bhaskaran, Appl Phys Lett 2014, 104.
[23] Y. C. Li, M. W. Lin, M. H. Yen, S. M. Fan, J. T. Wu, T. H. Young, J. Y. Cheng, S. J. Lin, ACS Appl Mater Interfaces 2015, 7, 22322.
[24] J. U. Lind, T. A. Busbee, A. D. Valentine, F. S. Pasqualini, H. Yuan, M. Yadid, S. J. Park, A. Kotikian, A. P. Nesmith, P. H. Campbell, J. J. Vlassak, J. A. Lewis, K. K. Parker, Nat Mater 2016.
[25] J. L. Tan, J. Tien, D. M. Pirone, D. S. Gray, K. Bhadriraju, C. S. Chen, Proc Natl Acad Sci U S A 2003, 100, 1484.
[26] Z. Liu, W. Li, X. Ma, N. Ding, F. Spallotta, E. Southon, L. Tessarollo, C. Gaetano, Y. S. Mukouyama, C. J. Thiele, J Biol Chem 2014, 289, 29801; J. Tchao, L. Han, B. Lin, L. Yang, K. Tobita, Sci Rep 2014, 4, 6614.
[27] S. R. Shin, H. Bae, J. M. Cha, J. Y. Mun, Y.-C. Chen, H. Tekin, H. Shin, S. Farshchi, M. R. Dokmeci, X. Tang, A. Khademhosseini, ACS Nano 2012, 6, 362.
[28] N. Tandon, C. Cannizzaro, P. H. Chao, R. Maidhof, A. Marsano, H. T. Au, M. Radisic, G. Vunjak-Novakovic, Nat Protoc 2009, 4, 155.
[29] J. W. Nichol, S. T. Koshy, H. Bae, C. M. Hwang, S. Yamanlar, A. Khademhosseini, Biomaterials 2010, 31, 5536.
[30] S. R. Shin, C. Zihlmann, M. Akbari, P. Assawes, L. Cheung, K. Zhang, V. Manoharan, Y. S. Zhang, M. Yuksekkaya, K. T. Wan, M. Nikkhah, M. R. Dokmeci, X. S. Tang, A. Khademhosseini, Small 2016, 12, 3677.

Figures and Figure captions

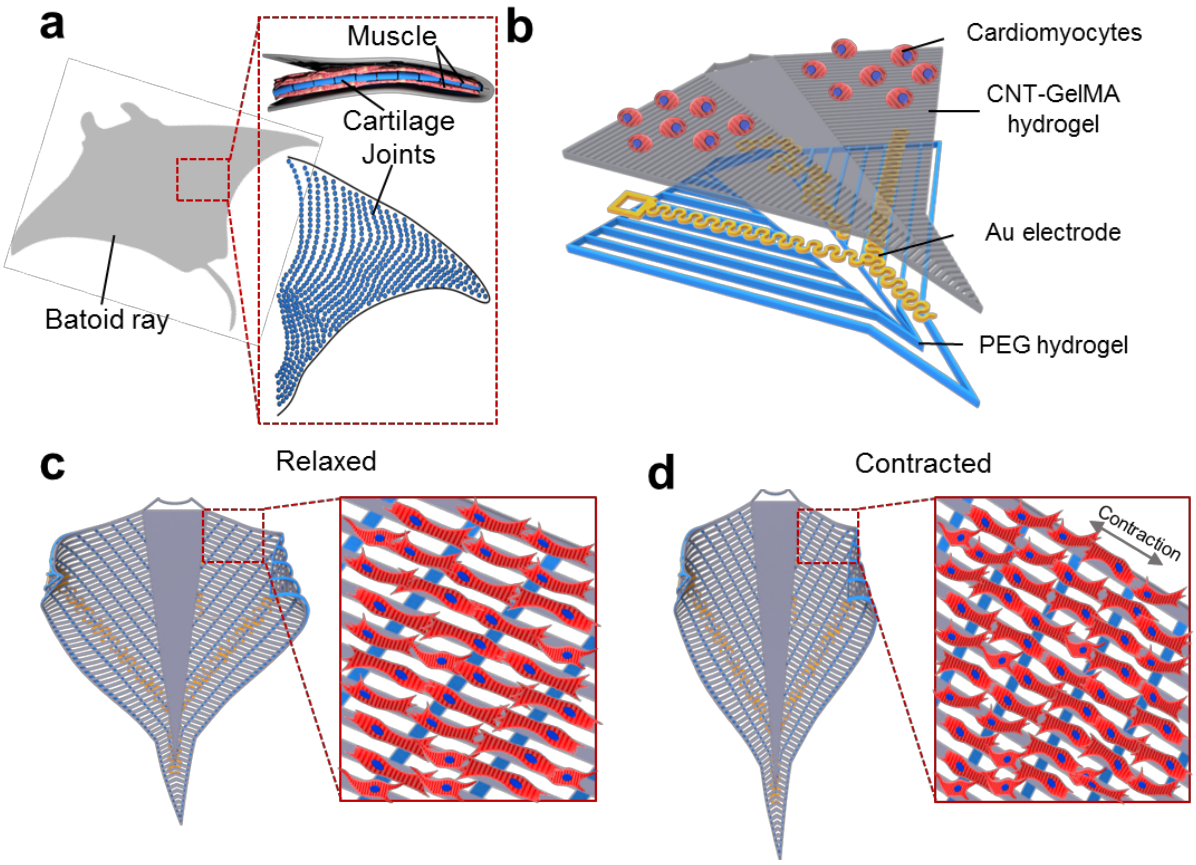

Figure 1. Schematic of the device. (a) Schematic of the cartilage joints and muscle pattern of a batoid ray fish. (b) Schematic illustration of the layer-by-layer structure of the construct. The bottom layer is composed of a PEG hydrogel with vertical patterned line alignment. The upper layer in contact with the cells is made of patterned CNT-GelMA hydrogel with a pattern, which is perpendicular to the PEG hydrogel pattern. The microelectrode network is embedded in between the two layers. (c, d) Schematic design of the batoid ray movement in the macro and micro scale: relaxed cardiomyocytes (c) and contracted cardiomyocytes (d).

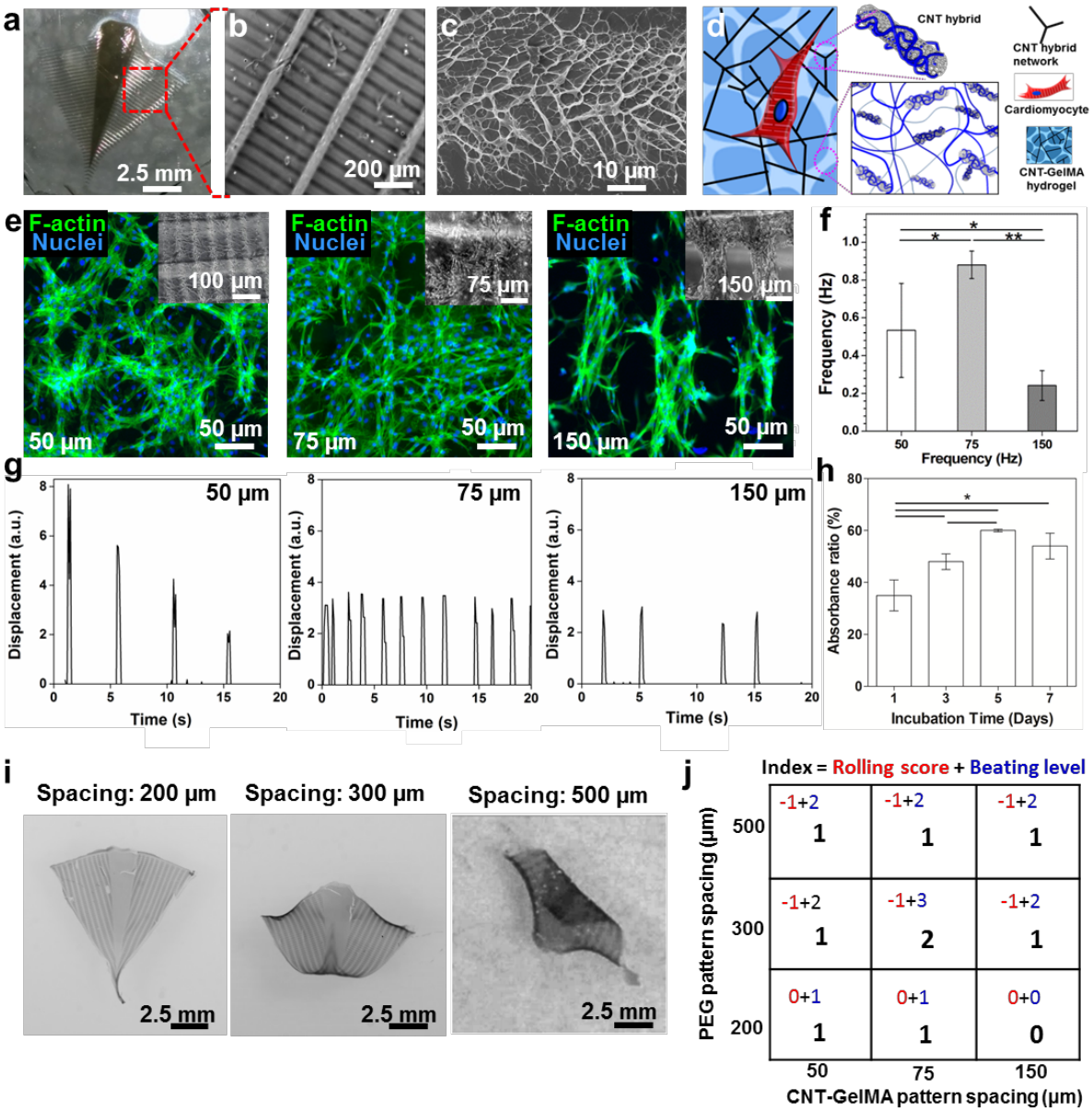

Figure 2. The optimization of PEG- and CNT-GelMA hydrogel patterns. (a) Image of the bio-inspired actuator without the Au microelectrode. (b) SEM image of the pattern of the dense CNT-GelMA hydrogel lines aligned perpendicular to the sparse PEG hydrogel lines. (c) SEM image of the fractal-like surface of the CNT-GelMA hydrogel pattern. (d) Schematic illustration of the CNTs embedded into the GelMA hydrogel. (e) Fluorescent images of cardiomyocytes on the CNT-GelMA hydrogel pattern at 50-, 75-, and 150-μm spacing. (f) Spontaneous beating frequency of cardiac tissues seeded on the multilayer bio-inspired actuator with different spacing between the CNT-GelMA hydrogel patterns on day 5. (*p< 0.05 and **p < 0.005) (h) Alamar blue assay of cardiomyocyte cultured on the bio-construct

after 7 days of incubation that revealed high cell viability. (*$p < 0.05$) (i) The rolling morphologies of the bio-inspired constructs with the PEG hydrogel pattern that is at 200-, 300-, and 500-μm spacing. (j) Table showing the index of the PEG hydrogel pattern and the CNT-GelMA hydrogel pattern optimization process: different spacing between the lines of PEG and CNT-GelMA hydrogels patterns have been inspected. For each device made with a different combination of patterns, the cell spreading, alignment, and beating behavior was analyzed. (Beating level indicated: 0, Very weak or no beating; 1, Weak beating; 2, Strong beating; 3, Very Strong beating. Rolling score indicated: -1, Rolling; 0, No Rolling).

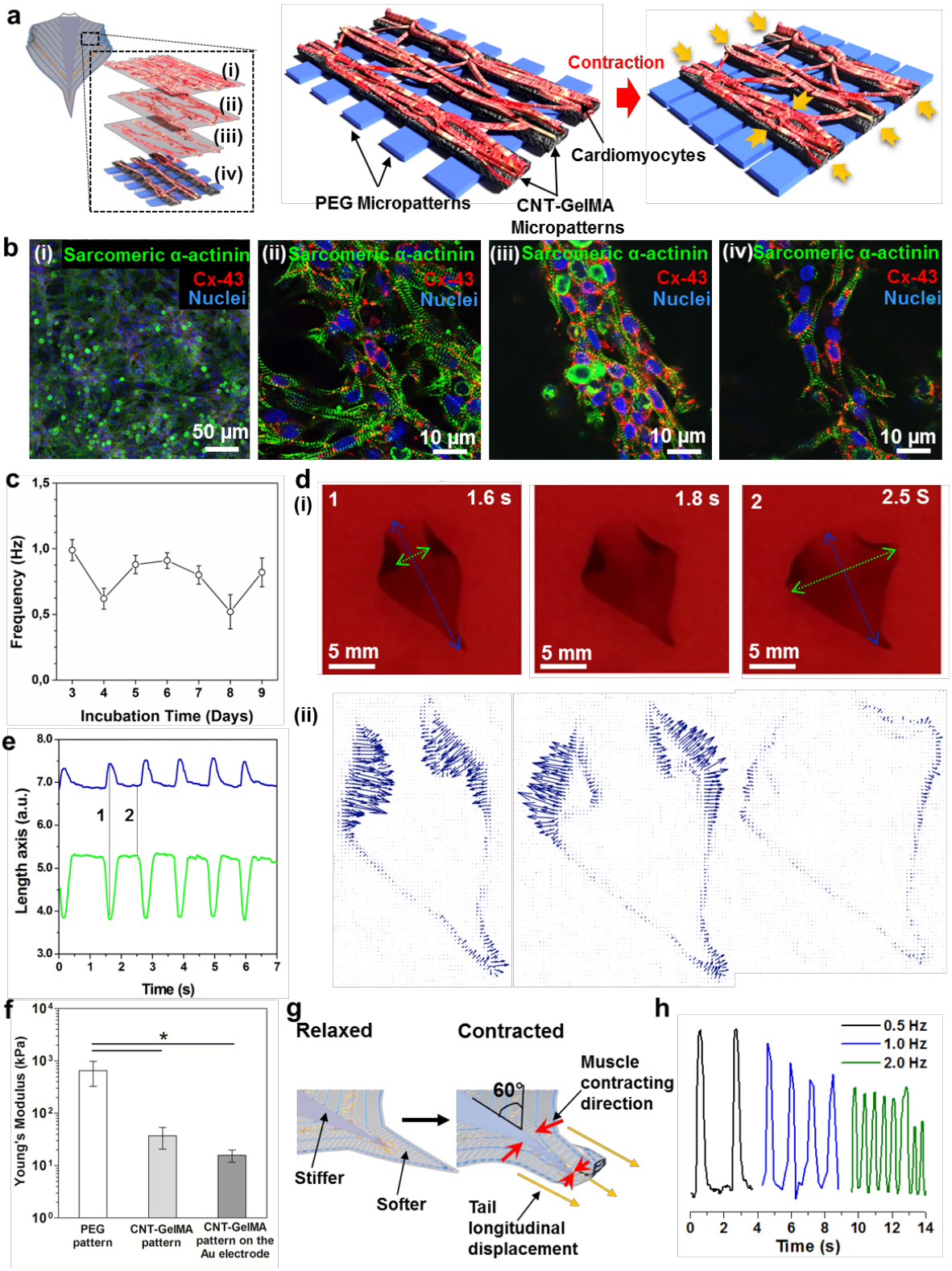

Figure 3. The characterization of the cardiomyocytes on the bio-inspired scaffold. (a) Schematic illustration of the contraction behavior of the cultured cardiac muscle tissue on the bio-inspired scaffold. (b) Confocal fluorescent images showed different morphology in the (i) upper, (ii) middle, and (iii, iv) bottom of cardiomyocytes cultured on the bio-inspired scaffold

for day 5. (c) Spontaneous beating rates of the cardiomyocytes on the bio-inspired scaffold from day 3 to day 9. (d) (i) Photograph of a free-standing bio-inspired soft robot cultured for 5 days at 0, 0.18, and 0.3 sec. The blue line represents the longitudinal axis displacement while the green line represents the transverse axis displacement. (ii) Particle Image Velocimetry measurement of the bio-inspired soft robot spontaneously moved within 0.3 sec. All arrows indicated direction and magnitude of beating motion. (e) Displacement of the two major axes during stimulated contractions (2 Hz, 1 V/cm). The blue line represents the longitudinal axis displacement (corresponding to the blue line in Figure 3d) while the green line (corresponding to the green line in figure 3d) represents the transverse axis displacement. The frame taken in correspondence to the lines marked with 1 and 2 are shown in Figure 3d. (f) Young's modulus of the PEG hydrogel pattern, CNT-GelMA hydrogel pattern, and the CNT-GelMA hydrogel pattern fabricated on the Au microelectrode. (*$p < 0.05$) (g) Schematic of the mechanism of tail longitudinal displacement which induces the soft robot displacement along the vertical direction, mainly on the tail part, when the cells contract. (h) Beating response of the bio-inspired soft robot when stimulated external AC electrical field at 1V/cm and with various frequencies from 0.5 to 2Hz.

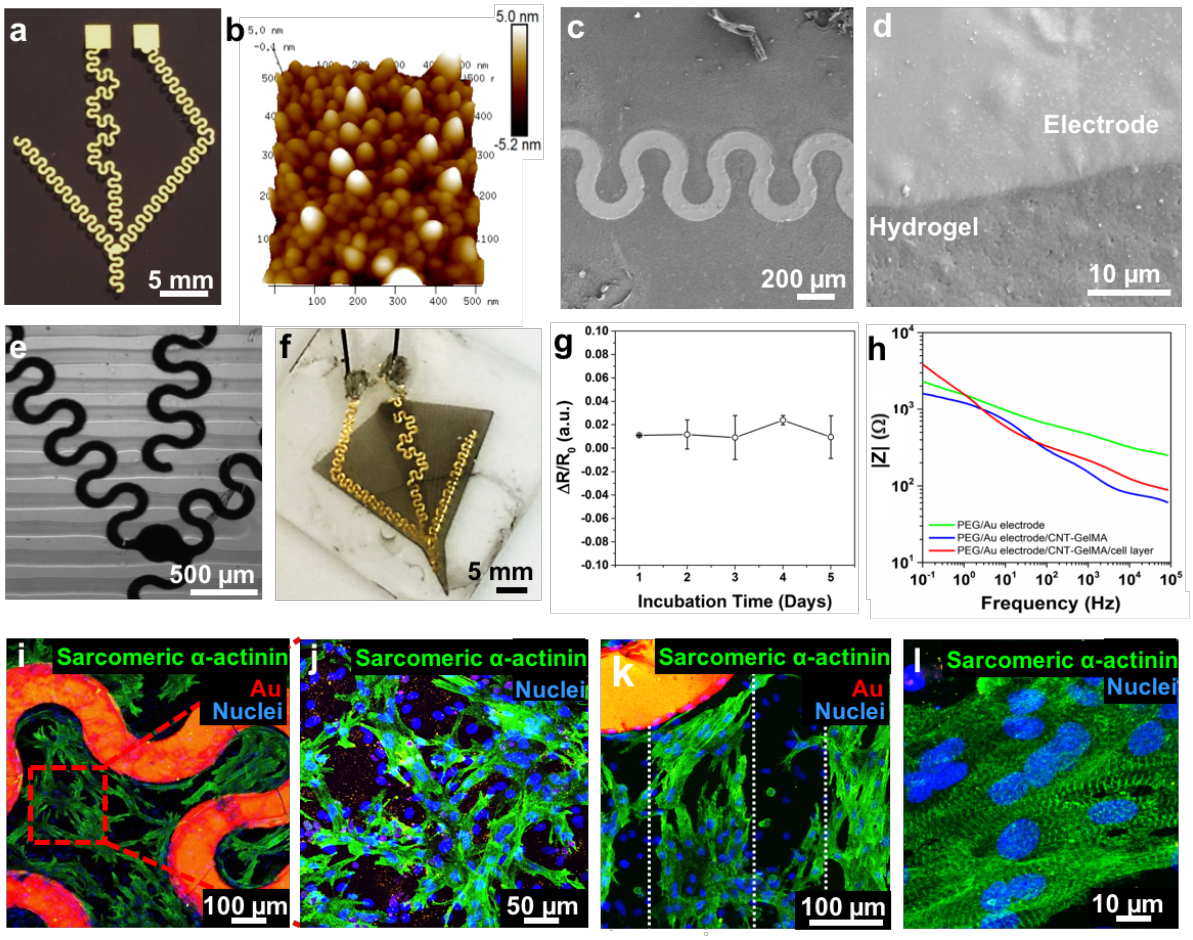

Figure 4. Characterization of the Au microelectrode and its incorporation into the bio-inspired soft robot. (a) E-beam-evaporated Au microelectrodes with a serpentine pattern. (b) AFM image of the bare Au microelectrodes. (c) and (d) SEM image of the Au microelectrode successfully transferred on the PEG hydrogel. (e) Optical microscope image of the Au microelectrodes successfully embedded in the CNT-GelMA hydrogel pattern. (f) Obtained bio-inspired soft robot with embedded Au microelectrodes. Copper wires were connected to the structure using silver paste as an electrical contact for local electrical stimulation. (g) Variation of the Au microelectrodes resistance embedded in the bio-inspired scaffold during 5 days of incubation in cell culture media at 37 °C. (h). Measured impedance modulus of Au microelectrodes transferred on the PEG hydrogel pattern (green), embedded in between PEG and CNT-GelMA hydrogel patterns (blue), and PEG and CNT-GelMA hydrogel patterns with cardiomyocytes layer (red). (i) Confocal fluorescence image of the cardiomyocytes, randomly spread among the Au microelectrodes (red signal) on the unpatterned central body. (j) The

cardiomyocytes exhibited a random network organization on the unpatterned central body. (k) Well-elongated and aligned cardiomyocytes were showed on the CNT-GelMA hydrogel pattern which is indicated by the white dots. (l) Partial uniaxial sarcomere alignment and interconnected sarcomeric structure was observed on the patterned areas.

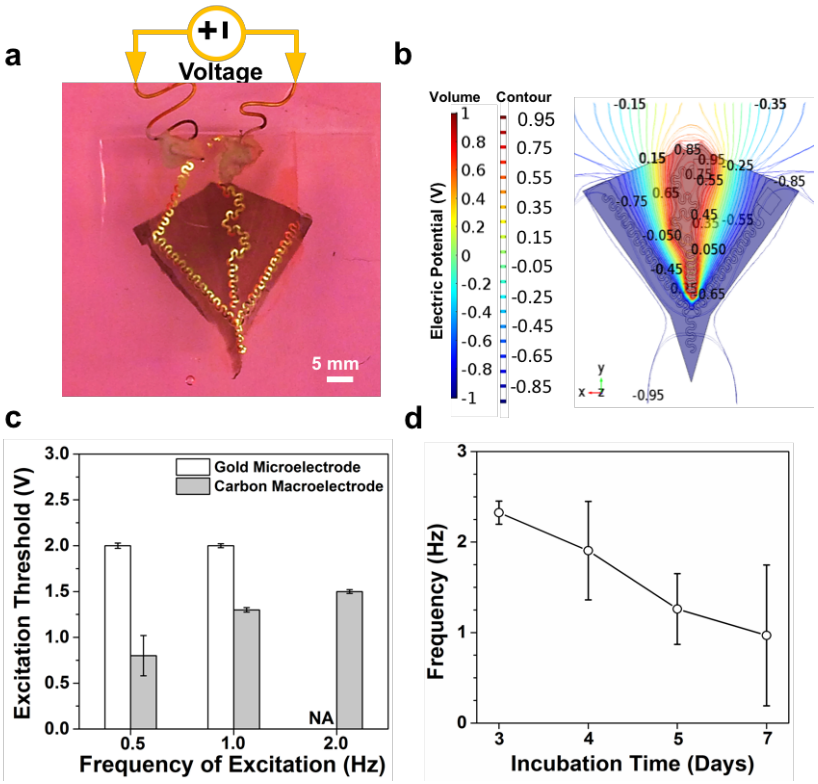

Figure 5. Electrical Stimulation of the bio-inspired soft robot. (a) Experimental setup used for the local electrical stimulation using the embedded Au microelectrodes connected to a waveform generator. (b) Top views of the numerically calculated electric potential contour plot volume distribution when a square wave signal (Peak Amplitude: 1 V, DC value: 0V, Frequency: 2 Hz, Pulse width: 50 ms, Duty Cycle: 10%) was applied to the embedded microelectrodes. (c) Excitation threshold voltage required at different frequencies (0,5 Hz, 1 Hz and 2 Hz), in the case of external carbon rod electrodes and embedded Au microelectrodes. (d) Spontaneous beating behavior of the bio-inspired soft robot with embedded Au microelectrodes after electrical stimulation.

Supporting Information

Title: Electrically Driven Microengineered Bio-inspired Soft Robots

By *Su Ryon Shin†*, Bianca Migliori†, Beatrice Miccoli, Yi-Chen Li, Pooria Mostafalu, Jungmok Seo, Serena Mandla, Alessandro Enrico, Silvia Antonia, Ram Sabarish, Ting Zheng, Pirrami Lorenzo, Yu Shrike Zhang, Kai-tak Wan, Demarchi Danilo, Mehmet R. Dokmeci, Ali Khademhosseini**

Supplementary figures

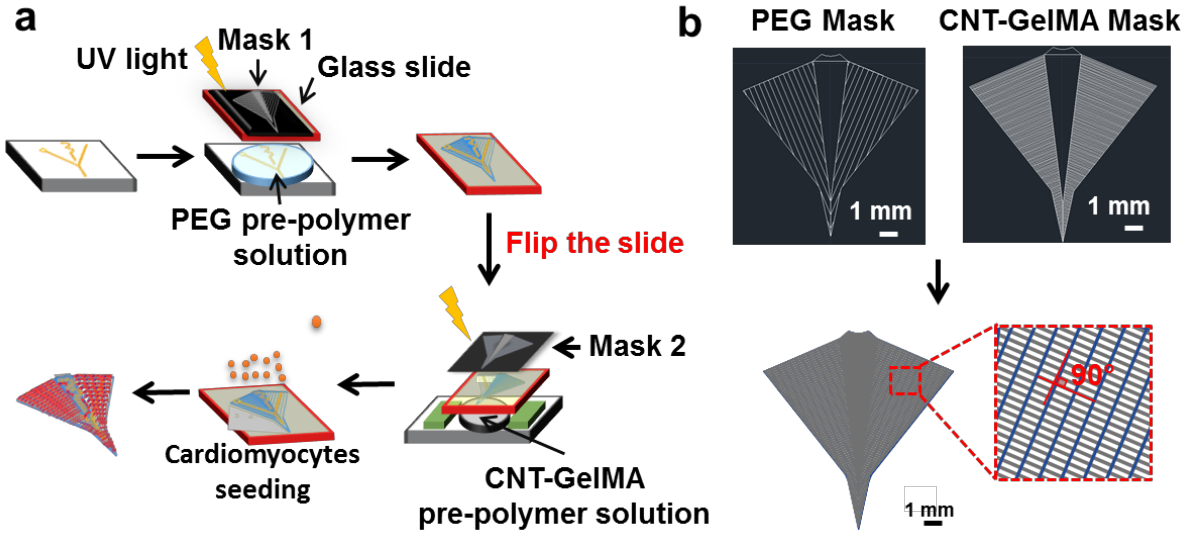

Figure S1. (a) The Au electrode is peeled from the glass slides thanks to the assistance of the PEG hydrogel layer directly UV-crosslinked on its surface through a specific photolithographic mask. The structure is then flipped, and a CNT-GelMA hydrogel pattern is crosslinked on the other electrode's surface. Cardiomyocytes are then seeded on the CNT-GelMA hydrogel top layer. The angle between the PEG and CNT-GelMA hydrogel pattern line was of 90°.

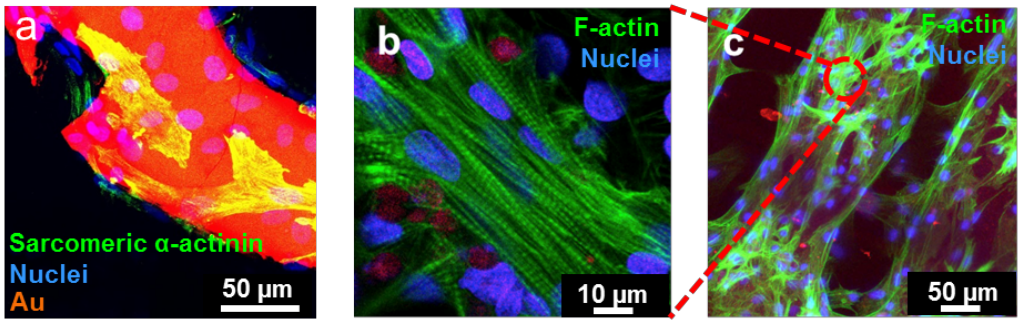

Figure S2. Confocal Microscope Images of the bio-inspired soft robot with embedded electrodes. (a) Confocal fluorescence images of cardiomyocytes on top of the embedded microelectrodes. The nuclei and sarcomeric α-actinin were observed as the pink and yellow color, as their original color was distorted following color channel merging with the strong red signal expression from the Au microelectrodes. (b-c) Confocal fluorescence images showed well-elongated cardiac cells and well-developed F-actin cross-striations along with the CNT-GelMA hydrogel pattern. F-actin and cell nuclei were labeled fluorescent green and blue, respectively.

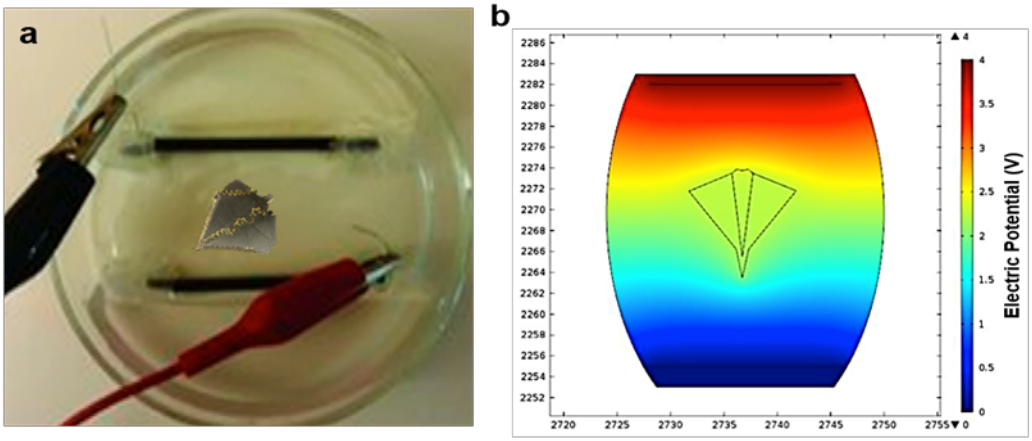

Figure S3. External Stimulation. Carbon rod electrodes (a) are used to externally stimulate the bio-inspired soft robot. In the case of external stimulation, the simulations reveal how the excitation voltage is almost uniformly distributed along the structure which implies an on/off displacement of the entire structure at the same time.

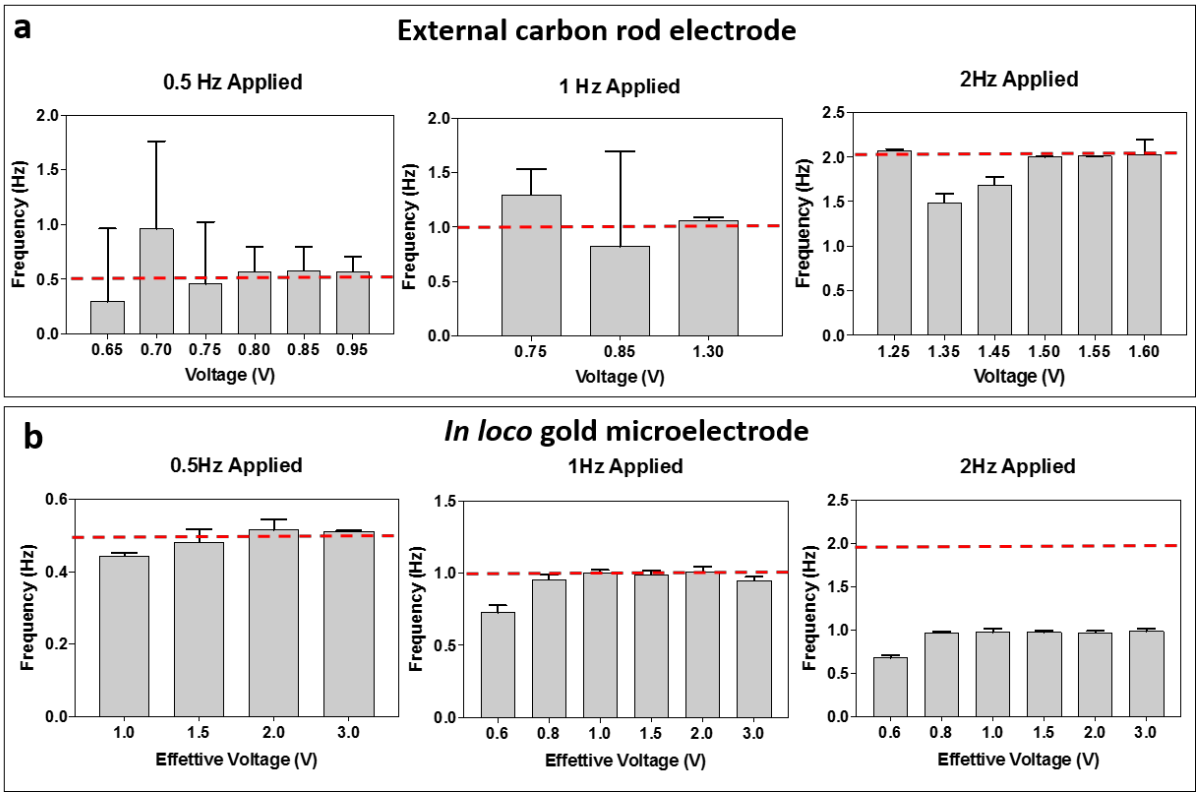

Figure S4. Excitation threshold voltage. The Excitation threshold voltage in the case of external carbon rod electrodes (a) and embedded Au microelectrodes (b) are shown when the applied frequency varied between 0.5, 1 and 2 Hz.

Video Recording of Actuators

File Name	Description
Video 1.mpg	Cardiomyocytes beating on the CNT-GelMA gel patterns (75 µm spacing)
Video 2.mpg	Beating behavior of bio-inspired construct with CNT-GelMA hydrogel pattern (75 µm spacing) and without PEG hydrogel pattern.

Video 3.mpg	Beating behavior of bio-inspired construct with CNT-GelMA hydrogel pattern (75 µm spacing) and PEG hydrogel pattern (200 µm spacing)
Video 4.mpg	Beating behavior of bio-inspired construct with CNT-GelMA hydrogel pattern (75 µm spacing) and PEG hydrogel pattern (300 µm spacing).
Video 5.mpg	Beating behavior of bio-inspired construct with CNT-GelMA hydrogel pattern (75 µm spacing) and PEG hydrogel pattern (500 µm spacing).
Video 6.mpg	Cardiomyocytes beating on the scaffold with Au microelectrode (75 µm spacing)

Local and external electrodes simulations details

A two-dimensional model was used to simulate the microengineered hydrogel structure both with embedded Au microelectrodes (Figure S5a) and without (Figure S5b). In the second case the electrical signal is applied through two Pt wires immersed in the cell culture media.

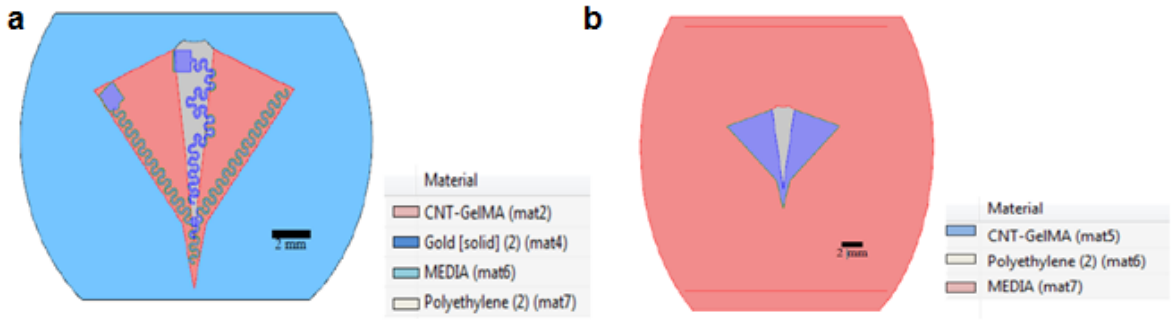

Figure S5. Simulation Geometry. 2D model used to simulate the bio-inspired soft robot (a) with and (b) without embedded Au microelectrodes.

In Table S1 are reported the conductivity and permittivity values considered for all the materials involved in the study.

Table S1. Materials parameters.

	Conductivity (S/m)	**Permittivity (F/m)**
Cell culture media	0.005	80
Au electrode	4×10^7	1
CNT-GelMA hydrogel with cardiomyocytes	0.2	20
PEG hydrogel layer	0.01	16

The partial differential equations (PDE) system used in the study is reported in Equation S1.

$$\begin{cases} \nabla \cdot J = Q_j \\ J = \sigma E + j\omega D + J_e \\ E = -\nabla V \end{cases}$$

Equation S1. Partial differential equations system.

Where J represents the current density, Q_j the charges present in the system, $D = \varepsilon_0 \varepsilon_r E$ the electric displacement, J_e the external charge density, and V the voltage.

The excitation voltage used is a square wave with parameters chosen according to the literature[1] and summarized in Table S2. In particular, the time between subsequent voltage pulses is chosen according to the human cardiac pace.

Table S2. Excitation signal specifications.

AC Peak Amplitude	4 V, external electrodes 2 V, embedded microelectrodes
Frequency	2 Hz
Pulses Interval	50 ms
Duty Cycle	10%
DC Offset	0 V

In the case of local electrical stimulation, the amplitude of the peak voltage signal is decreased from 4 V to 2 V as the signal is directly applied to the microengineered hydrogel.

The results of external and local stimulation are reported in Figure S4b and 5c, respectively. In the case of the external electrodes, there is almost no potential difference along the bioactuator structure, thus implying that all the cardiomyocytes will contract at the

same time, while, when the in the case of embedded microelectrodes, the signal propagates along the structure, leading to a wave-like beating behavior.

References

[1] J.P. Spatz, Nat. Mater. 2005, 4, 115–116.